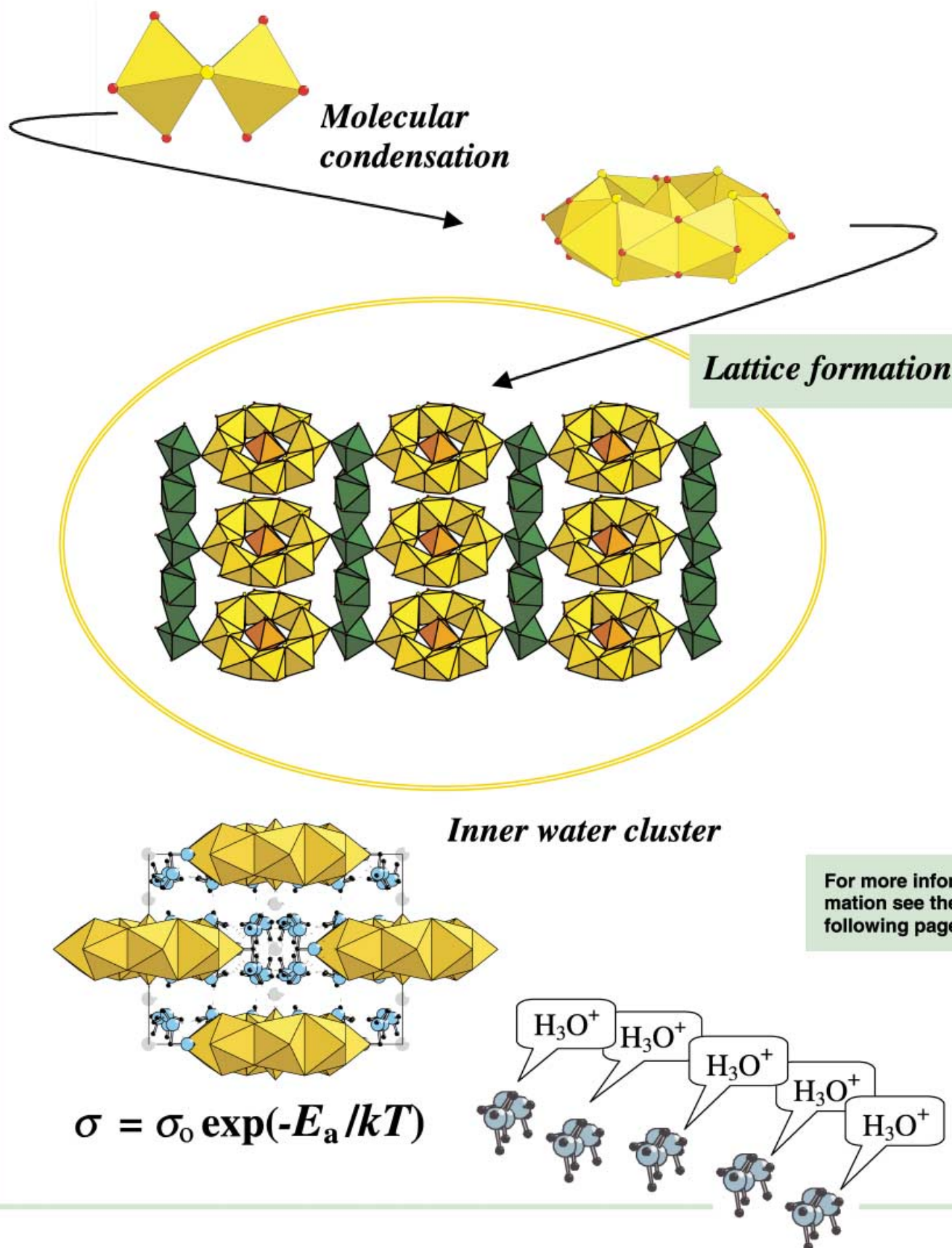


Molecular 3D protonic conductor



Synthesis, X-ray and Neutron Diffraction Characterization, and Ionic Conduction Properties of a New Oxothiomolybdate $\text{Li}_3[\text{Mo}_8\text{S}_8\text{O}_8(\text{OH})_8\{\text{HWO}_5(\text{H}_2\text{O})\}] \cdot 18\text{H}_2\text{O}$

Anne Dolbecq,*^[a] Charlotte du Peloux,^[a] Anne-Laure Auberty,^[a] Sax A. Mason,^[b] Philippe Barboux,^[c] Jérôme Marrot,^[a] Emmanuel Cadot,^[a] and Francis Sécheresse^[a]

Abstract: The new oxothiomolybdate anion $[\text{Mo}_8\text{S}_8\text{O}_8(\text{OH})_8\{\text{HWO}_5(\text{H}_2\text{O})\}]^{3-}$ (denoted $\text{HMo}_8\text{W}^{3-}$) has been synthesized in aqueous solution by an acido–basic condensation reaction. Four $\{\text{Mo}^{\text{V}}_2\text{S}_2\text{O}_2\}$ building blocks are connected through hydroxo bridges around a central $\{\text{W}^{\text{VI}}\text{O}_6\}$ octahedron. X-ray and neutron diffraction studies have been performed on single crystals of the lithium salt $\text{Li}_3[\text{Mo}_8\text{S}_8\text{O}_8(\text{OH})_8\{\text{HWO}_5(\text{H}_2\text{O})\}] \cdot 18\text{H}_2\text{O}$ ($\text{Li}_3\text{HMo}_8\text{W} \cdot 18\text{H}_2\text{O}$) grown from $\text{HMo}_8\text{W}^{3-}$ in an aqueous

solution of LiCl (1M). The neutron diffraction experiment enabled us to locate both the protons and the lithium ions. In the structure of $\text{Li}_3\text{HMo}_8\text{W} \cdot 18\text{H}_2\text{O}$, ring-shaped anions interleaved by a cluster of disordered hydrogen-bonded water molecules stack on top of each other along lithium pillars. The

Keywords: ionic conductivity • lithium • molybdenum • neutron diffraction • polyoxometalates

lithium columns are formed by alternating edge-sharing octahedra and tetrahedra, with one lithium site in four being totally vacant. Ionic conductivity measurements on pressed pellets have shown that $\text{Li}_3\text{HMo}_8\text{W} \cdot 18\text{H}_2\text{O}$ is a good ionic conductor at room temperature ($\sigma = 10^{-5} \text{ S cm}^{-1}$), but the ionic conductivity on single crystals is smaller by two orders of magnitude and is isotropic; this suggests the main path of conduction involves surface protons rather than lithium ions of the bulk.

Introduction

The synthesis of polyoxometalates is mainly based on acido–basic condensation.^[1] Most of these anions have discrete structures of definite sizes and shapes belonging to well-known structural types, such as the Lindquist (e.g., $[\text{Mo}_6\text{O}_{19}]^{2-}$), Keggin (e.g., $[\text{PMo}_{12}\text{O}_{40}]^{3-}$) or Dawson (e.g., $[\text{P}_2\text{Mo}_{18}\text{O}_{62}]^{6-}$) types. One strategic route to increase the nuclearity of polyoxometalates and reach nanometric size consists of the introduction of reduced metal centers into polyanionic frameworks. The resulting enhanced nucleophilic character of the polyanion allows stereospecific reactions with electrophilic fragments and produces novel and larger poly-

oxometalates.^[2, 3] Another way to design new structural arrangements is to use sulfur-enriched precursors. Sulfur in the coordination sphere of a metal atom is expected to modify its reactivity, and thus the aggregation processes of the elemental building units during the condensation reaction and also to provide new connectivity schemes between the constituent metal polyhedra. We have recently developed a synthetic strategy based on the self-condensation of $\{\text{Mo}^{\text{V}}_2\text{S}_2\text{O}_2\}$ structural units. The addition of hydroxide ions to an aqueous solution of $[\text{Mo}_2\text{S}_2\text{O}_2(\text{H}_2\text{O})_6]^{2+}$ dithiocations gives, at a pH below 3, a yellow solid,^[4] which affords, after recrystallization, the neutral cyclic derivative $[\text{Mo}_{12}\text{S}_{12}\text{O}_{12}(\text{OH})_{12}(\text{H}_2\text{O})_6]$,^[5] the first member of a new original family of compounds. The crude product regenerates the thioanion in acid media and hydrolyzes in basic media to give the $[\text{Mo}_2\text{S}_2\text{O}_2(\text{OH})_4(\text{H}_2\text{O})_2]^{2-}$ ion, and is therefore a convenient precursor for further condensation reactions. The efficiency of the synthetic procedure has been demonstrated by the synthesis of a large variety of cyclic oxothioanions, either template-free,^[5] or incorporating dicarboxylate molecules^[6] or phosphate ions.^[7] These anions crystallize with alkaline cations to form columns, planes, or even three-dimensional structures^[8] that can confer interesting physical properties such as ionic conductivity or microporosity.^[9] In a previous communication, we showed that inorganic structuring agents such as molybdate ions could also be used to prepare cyclic

[a] Dr. A. Dolbecq, C. du Peloux, Dr. A.-L. Auberty, Dr. J. Marrot, Dr. E. Cadot, Prof. Dr. F. Sécheresse
Institut Lavoisier, IREM, UMR 8637
Université de Versailles Saint-Quentin
45 Avenue des Etats-Unis, 78035 Versailles cedex (France)
Fax: (+33) 139-254381
E-mail: dolbecq@chimie.uvsq.fr

[b] Dr. S. A. Mason
Institut Laue-Langevin, BP 156
38042 Grenoble cedex 9 (France)

[c] Dr. P. Barboux
Physique de la Matière Condensée
Ecole Polytechnique
CNRS-UMR 7643C, 91128 Palaiseau cedex (France)

oxothio compounds.^[10] Then, we extended this synthetic protocol to tungstate ions, and we report herein the synthesis and complete characterization of the oxothioanionic wheel $[\text{Mo}_8\text{S}_8\text{O}_8(\text{OH})_8\{\text{HWO}_5(\text{H}_2\text{O})\}]^{3-}$ denoted below as $\text{HMo}_8\text{W}^{3-}$. This compound exhibits a remarkable three-dimensional structure in which wheels that contain anionic planes are interleaved by partly filled lithium columns. By using single-crystal neutron diffraction, not only have the protons been located, but the occupation factors of the lithium cations have also been determined. The protons appear distributed over the inorganic wheel as hydroxyl groups and spread in the lattice holes as water molecules overlapping in a sophisticated H-bonding network.

Results and Discussion

Synthesis of $\text{HMo}_8\text{W}^{3-}$: The synthesis of the polyoxothioanion is quite straightforward, starting from a basic aqueous solution of tungstate ions and with a stoichiometric Mo/W ratio. The molybdenum oxothioprecursor^[4, 5] is then added and dissolves to give the red anionic dinuclear compound $[\text{Mo}_2\text{S}_2\text{O}_2(\text{OH})_4(\text{H}_2\text{O})_2]^{2-}$. The condensation of the dianion around the inorganic template monomer is induced by the addition of hydrochloric acid until $\text{pH} = 4.5$. The $\text{HMo}_8\text{W}^{3-}$ ion is isolated in the solid state as the potassium salt $\text{K}_3[\text{Mo}_8\text{S}_8\text{O}_8(\text{OH})_8\{\text{HWO}_5(\text{H}_2\text{O})\}] \cdot 18\text{H}_2\text{O}$ ($\text{K}_3\text{HMo}_8\text{W} \cdot 18\text{H}_2\text{O}$). Single crystals as large as 2 mm^3 of the lithium salt $\text{Li}_3[\text{Mo}_8\text{S}_8\text{O}_8(\text{OH})_8\{\text{HWO}_5(\text{H}_2\text{O})\}] \cdot 18\text{H}_2\text{O}$ ($\text{Li}_3\text{HMo}_8\text{W} \cdot 18\text{H}_2\text{O}$) are easily grown by slow evaporation of an aqueous solution of LiCl (ca. 1 M) that contains $\text{HMo}_8\text{W}^{3-}$.

Molecular structure of $\text{HMo}_8\text{W}^{3-}$ in $\text{Li}_3\text{HMo}_8\text{W} \cdot 18\text{H}_2\text{O}$: Four $\{\text{Mo}_2\text{S}_2\text{O}_2\}$ building blocks are connected by hydroxo bridges and encapsulate a central $\text{W}^{\text{VI}}\text{O}_6$ octahedron (Figure 1). As the anion sits on an inversion center, the central metal atom is disordered over two positions, located 0.35 Å above and below the plane defined by the molybdenum atoms of the octanuclear wheel. Each molybdenum atom of the ring exhibits a distorted octahedral coordination (Figure 1a, Table 1). The octahedra are alternately face-sharing (between the building units) and edge-sharing (within the building units), a common feature with the parent neutral $[\text{Mo}_{12}\text{S}_{12}\text{O}_{12}(\text{OH})_{12}(\text{H}_2\text{O})_6]$ wheel^[5] and the octanuclear $[\text{Mo}_8\text{S}_8\text{O}_8(\text{OH})_8(\text{C}_2\text{O}_4)]^{2-}$ ion.^[6] The central WO_6 octahedron shares four corners with the four $\{\text{Mo}_2\text{S}_2\text{O}_2\}$ units.

Proton distribution in $\text{HMo}_8\text{W}^{3-}$ by neutron diffraction: The hydrogen atoms on the hydroxo bridges, H3A and H3B, are directed above and below the molecular plane. The octanuclear ring $\{\text{Mo}_8\text{S}_8\text{O}_8(\text{OH})_8\}$ being neutral, and the central $\text{W}^{\text{VI}}\text{O}_6$ octahedron having a formal -6 charge, three additional protons have to be located on the polyoxothioanion in order to satisfy the overall -3 charge of the anion. The three additional protons are localized on the oxygen atoms of the central WO_6 octahedron. There are three sets of W–O bond lengths within the WO_6 octahedron (Table 1). One $\text{W1C}–\text{O1C}$ bond (1.715(6) Å) is short and is attributed to a

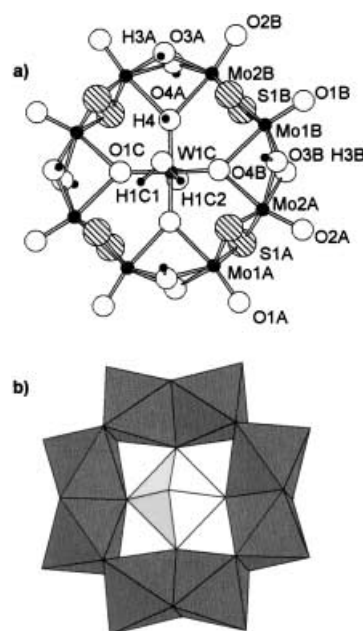


Figure 1. a) Ball and stick representation and atom-labeling scheme of the $[\text{Mo}_8\text{S}_8\text{O}_8(\text{OH})_8\{\text{HWO}_5(\text{H}_2\text{O})\}]^{3-}$ ion; the asymmetric unit consists of a quarter of a polyoxothioanion, with two fragments labeled A and B. b) Polyhedral representation showing the connectivity of the building blocks; disordered hydrogen atoms generated by the C_2 axis and the mirror have been omitted for clarity.

Table 1. Selected bond lengths [Å] in $\text{Li}_3\text{HMo}_8\text{W} \cdot 18\text{H}_2\text{O}$.

	X-ray	Neutron		X-ray	Neutron
Mo1A–O1A	1.696(5)	1.693(5)	Mo1B–O1B	1.697(5)	1.687(4)
Mo1A–O3A	2.090(4)	2.101(4)	Mo1B–O3B	2.093(3)	2.099(4)
Mo1A–S1A	2.316(1)	2.313(5)	Mo1B–S1B	2.318(1)	2.315(6)
Mo1A–O4A	2.381(5)	2.375(5)	Mo1B–O4B	2.403(5)	2.394(6)
Mo1A–Mo2A	2.8013(8)	2.802(4)	Mo1B–Mo2B	2.8047(8)	2.805(4)
Mo2A–O2A	1.688(5)	1.691(4)	Mo2B–O2B	1.673(5)	1.683(4)
Mo2A–O3B	2.123(3)	2.128(4)	Mo2B–O3A	2.111(4)	2.114(4)
Mo2A–O4B	2.219(4)	2.231(4)	Mo2B–S1B	2.316(1)	2.311(6)
Mo2A–S1A	2.319(1)	2.317(5)	Mo2B–O4A	2.336(5)	2.347(4)
W1C–O1C	1.715(6)	1.732(8)	W1C–O4B	1.875(4)	1.879(3)
W1C–O1C	2.464(6)	2.467(6)	W1C–O4A	1.966(5)	1.962(4)
Li1–O1AW	1.995(12)	1.984(11)	Li1–O1BW	1.941(11)	1.957(9)
Li2A–O2A	2.052(5)	2.051(4)	Li2B–O2B	2.134(5)	2.143(4)
Li2A–O1AW	2.175(4)	2.185(3)	Li2B–O1BW	2.205(4)	2.202(5)
Li1–Li2A	2.95(2)	2.93(2)	Li1–Li2B	2.62(2)	2.64(2)

W=O bond while the other is far longer (2.464(6) Å) and is characteristic of a terminal aqua bond. The values observed here are even slightly longer than those reported for terminal W–OH₂ ligands *trans* to oxo groups,^[11] suggesting the weak nature of the binding of the aqua ligand in these species. Accordingly, two disordered hydrogen atoms, H1C1 and H1C2 (Figure 1a), have been located in the neutron Fourier difference maps. The third proton, H4, located on the triply bridging oxygen atoms, is delocalized on the two equivalent positions O4A, in agreement with the W–O bond lengths. Indeed, among the four equatorial $\text{W1C}–\text{O}$ bonds, one set of bond lengths ($\text{W1C}–\text{O4A} = 1.966(5)$ Å) is significantly longer than the other ($\text{W1C}–\text{O4B} = 1.875(4)$ Å), as expected for a W–OH bond. Polyanionic structures with protonated $\mu_3\text{-O}$ atoms are not uncommon, the best-known example being the structure of the metatungstate $[\text{W}_{12}\text{O}_{38}(\text{OH})_2]^{6-}$ ion.^[12]

Three-dimensional structure of $\text{Li}_3\text{HMo}_8\text{W} \cdot 18\text{H}_2\text{O}$: In the structure of $\text{Li}_3\text{HMo}_8\text{W} \cdot 18\text{H}_2\text{O}$, anions and cations are mutually connected. Three crystallographically independent positions for the lithium atoms were located unambiguously by X-ray diffraction, Li1, Li2A, and Li2B. Li1 has regular tetrahedral coordination, while Li2A and Li2B are octahedrally coordinated (Table 1). The coordination sphere of the cations is formed by terminal oxo ligands of the polyanion and by aquo ligands (Figure 2a). Indeed, both tetrahedral^[13] and

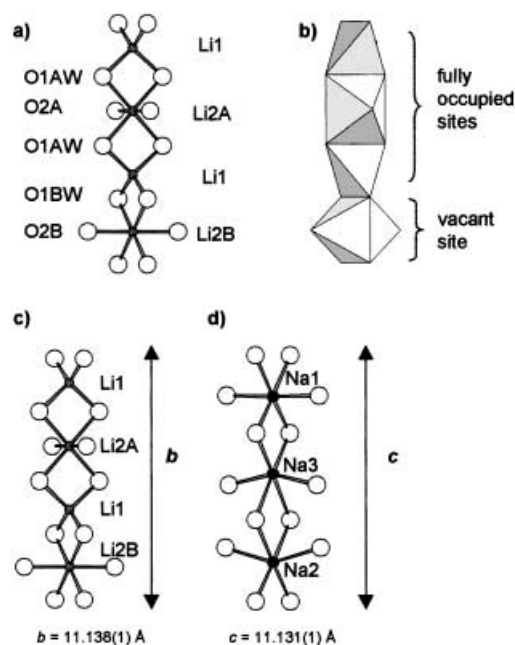


Figure 2. a) Ball and stick representation of the repeating motif of the lithium columns in $\text{Li}_3\text{HMo}_8\text{W} \cdot 18\text{H}_2\text{O}$ with the lithium occupancies. b) Polyhedral representation showing the alternation of edge-sharing octahedra and tetrahedra. Comparison of c) the lithium columns in $\text{Li}_3\text{HMo}_8\text{W} \cdot 18\text{H}_2\text{O}$ and d) the sodium columns in $\text{Na}_4[(\text{HPO}_4)_2\text{Mo}_{12}\text{S}_{12}\text{O}_{12}(\text{OH})_{12}(\text{H}_2\text{O})_2] \cdot 27\text{H}_2\text{O}$.^[7b]

octahedral^[14] coordination are equally encountered among lithium complexes with oxygen donor ligands. The lithium octahedra and tetrahedra are alternately connected to each other by sharing edges, thus forming a spectacular infinite lithium column (Figure 2b) with short $\text{Li} \cdots \text{Li}$ separations (2.64(2)–2.95(2) Å; Table 1). This one-dimensional chain is comparable to the cationic arrangement in $\text{Na}_4[(\text{HPO}_4)_2\text{Mo}_{12}\text{S}_{12}\text{O}_{12}(\text{OH})_{12}(\text{H}_2\text{O})_2] \cdot 27\text{H}_2\text{O}$.^[7b] In this compound, sodium pillars are formed by edge-sharing sodium octahedra. The repeating unit in the sodium columns (Figure 2d) consists of three edge-sharing octahedra and corresponds to the *c* parameter (11.135(1) Å) of the orthorhombic cell, while in $\text{Li}_3\text{HMo}_8\text{W} \cdot 18\text{H}_2\text{O}$, the repeating motif is formed by four lithium polyhedra (Figure 2c) and corresponds to the *b* crystallographic parameter with approximately the same length ($b = 11.138(1)$ Å). Some electron density was found by X-ray diffraction in the lithium site Li2B. However, the neutron diffraction experiment showed unambiguously that this site was totally vacant, the other sites in the repeating motif (Li1, Li2A) being fully occupied. To our knowledge, this is the first lithium compound with alternating octahedra and

tetrahedra forming lithium pillars. Infinite lithium chains are often encountered among inorganic structures, but consist only of octahedra or tetrahedra. For example, in the structure of lithium hydroxide, Li is tetrahedrally coordinated by two hydroxo ligands and two water molecules and each tetrahedron shares an edge and two corners to produce double chains.^[15] Besides, in most inorganic lithium salts, Li is coordinated by six water molecules to form chains of face-sharing octahedra.^[15]

The Li2A and Li2B cations connect one polyanion to four others through the terminal oxygen atoms O2A and O2B, thus forming a regular planar grid (Figure 3a). The mixed anionic–cationic planes stack on top of each other, each plane being shifted from the following one by $a/2$ so that one hole of the grid is facing a polyanion of the planes above and below. The anions are anchored to the lithium columns as shown in Figure 3b.

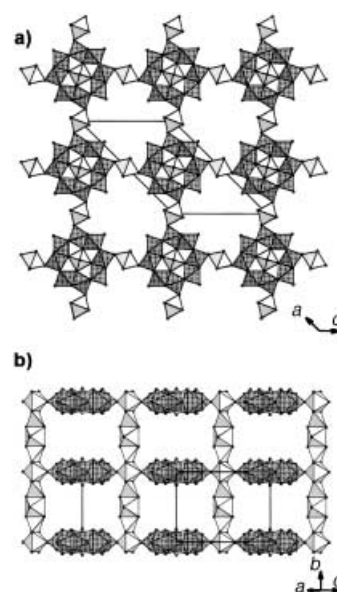


Figure 3. a) View of the grid formed by anions connected to each other by lithium octahedra in the (010) planes. b) View of the packing of the anions along the lithium pillars in the (101) planes.

Hydrogen-bonding interactions: Three kinds of water molecules have been found in the structure of $\text{Li}_3\text{HMo}_8\text{W} \cdot 18\text{H}_2\text{O}$: water molecules (O1W and O1BW) attached to the lithium ions, representing eight molecules among the 18; water molecules (O2AW, O2BW) located above and below the hydroxo groups, representing eight molecules; and two molecules disordered over three sites (O3AW, O3BW, and O3CW). All the protons of the structure have been located in Fourier difference maps, some of them being disordered over two positions. Each hydrogen atom of the water molecules is involved in an $\text{O} \cdots \text{O}$ hydrogen bond (Table 2). Hydrogen-bonding interactions are also found between the bridging oxygen atoms (O3A, O3B) of the oxothioanion and the water molecules located above and below the molecular plane (Figure 4a). The geometry of the hydrogen bonds is characteristic of moderately strong interactions^[16] with $\text{O3A} \cdots \text{O2AW}$ and $\text{O3B} \cdots \text{O2BW}$ distances of 2.68(1) and 2.70(1) Å, re-

Table 2. Geometrical parameters of the hydrogen bonds in $\text{Li}_3\text{HMo}_8\text{W}\cdot 18\text{H}_2\text{O}$ determined by neutron diffraction between donor oxygen atoms (D) and acceptor oxygen atoms (A).

D–H...A	<i>d</i> (D–H)	<i>d</i> (H...A)	<i>d</i> (D...A)	∠DHA
donor oxygen atoms of the polyoxothioanion				
O1C–H1C1...O3AW	1.10(4)	2.16(4)	2.81(2)	115(2)
O1C–H1C2...O3BW	1.06(4)	2.27(4)	2.83(2)	111(2)
O3A–H3A...O2AW	0.97(1)	1.73(1)	2.68(1)	166.5(5)
O3B–H3B...O2BW	0.98(1)	1.74(1)	2.70(1)	165.4(5)
O4A–H4...O1C	1.12(3)	2.06(2)	2.85(1)	124(1)
donor oxygen atoms of the water molecules				
O1AW–H1A1...O3B	0.95(1)	1.85(1)	2.78(5)	164.1(5)
O1AW–H1A2...O2AW	0.93(1)	1.87(1)	2.80(1)	169.9(6)
O1BW–H1B1...O3A	0.96(1)	1.89(1)	2.81(1)	161.5(7)
O1BW–H1B2...O2BW	0.91(2)	1.96(2)	2.85(7)	162(1)
O2AW–H2A1...O1A	0.89(2)	2.08(2)	2.96(1)	168(2)
O2AW–H2A2...O3BW	0.93(3)	1.78(3)	2.67(2)	159(3)
O2AW–H2A3...O3CW	1.03(2)	1.88(3)	2.80(3)	147(1)
O2AW–H2A4...O1A	0.97(2)	2.20(2)	2.96(1)	134(1)
O2BW–H2B2...O1BW	0.93(3)	1.93(3)	2.85(1)	168(2)
O3AW–H3A1...O2BW	1.02(5)	1.97(4)	2.97(1)	164(3)
O3AW–H3A2...O1C	1.00(5)	1.81(4)	2.81(2)	175(3)
O3BW–H3B1...O1C	1.03(4)	1.81(3)	2.83(2)	166(3)
O3CW–H3C1...O1B	0.94(7)	1.93(5)	2.86(4)	170(4)

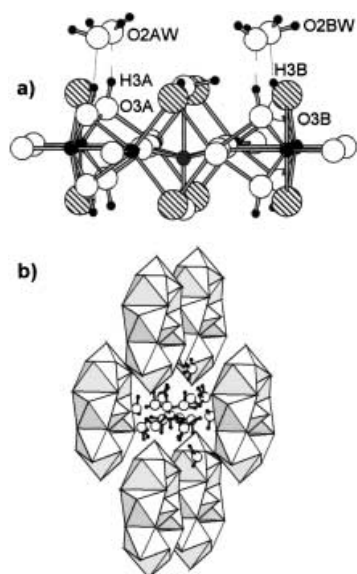


Figure 4. a) Side view of the anion showing the hydrogen bonds between the hydroxo groups and water molecules. b) View of the cluster of disordered water molecules hydrogen-bonded to six adjacent polyoxothioanions; hydrogen bonds have been omitted for clarity.

spectively, and O3A–H3A...O2AW and O3B–H3B...O2BW angles of 166.5(5) and 165.4(5)°, respectively (Table 2). The water molecules O1AW and O1BW linked to the lithium atoms are hydrogen-bonded to the bridging oxygen atoms O3A and O3B of the anion and also to the O2AW and O2BW water molecules (Table 2). Finally, a water molecule disordered over three positions O3AW, O3BW, and O3CW acts as donor and acceptor of hydrogen

bonds with the terminal oxygen atom O1C of the anion and the remaining water molecules (Table 2). The cluster of hydrogen-bonded water molecules thus formed fits in the cavities defined by six adjacent polyanions (Figure 4b), and the intricate hydrogen bonding pattern participates to the cohesion of the whole structure.

Thermal behavior: The thermal behavior of $\text{Li}_3\text{HMo}_8\text{W}\cdot 18\text{H}_2\text{O}$ was studied by X-ray powder diffraction and thermogravimetric analysis (TGA) upon heating. The TGA curve (Figure 5) shows two successive mass losses of about two

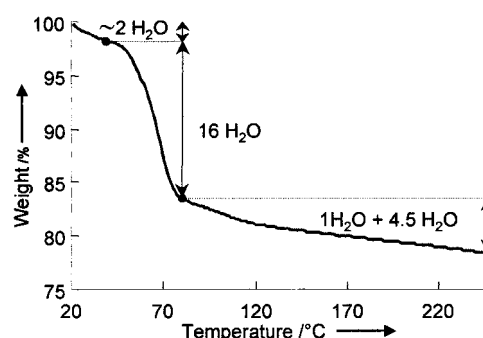


Figure 5. Thermogravimetric analysis (TGA) curve of $\text{Li}_3\text{HMo}_8\text{W}\cdot 18\text{H}_2\text{O}$.

water molecules (between 20 and 40°C), which could correspond to the disordered O3W molecules and followed by sixteen water molecules (between 40 and 75°C) attributed to the sixteen O1AW, O1BW, O2AW, and O2BW molecules. The last weight loss involves the water molecule O1C bound to the W atom followed by hydroxo groups. In the range 25–100°C, $\text{Li}_3\text{HMo}_8\text{W}\cdot 18\text{H}_2\text{O}$ undergoes one phase transition at 65°C, as shown by the evolution of the powder X-ray diffraction patterns (Figure 6), corresponding to the loss of the hydration water molecules. The orange powder turns brown upon heating. The X-ray powder diffraction pattern of a sample heated for one hour at 100°C and cooled to room temperature over one hour is similar to the initial powder pattern, showing the phase transition is reversible, as confirmed also by the return to the original orange color of the sample.

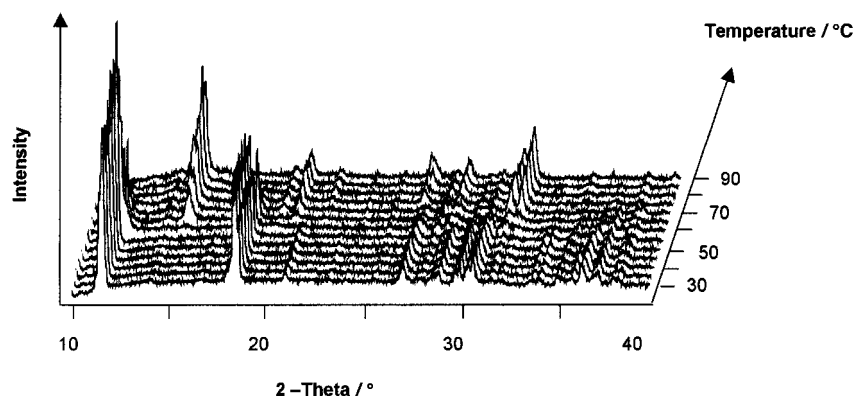


Figure 6. Thermodiffractograms taken on heating $\text{Li}_3\text{HMo}_8\text{W}\cdot 18\text{H}_2\text{O}$ in air.

Ionic conductivity measurements: Considering the three-dimensional structure of $\text{Li}_3\text{HMo}_8\text{W}\cdot 18\text{H}_2\text{O}$, two kinds of mobile ions can be identified. The most obvious ones are the lithium ions. Indeed, the lithium columns are only partially filled, therefore hopping of lithium ions from one occupied site to an adjacent vacant site in the column can be considered. The crystallographic b axis would be the main conducting path. By comparison with related compounds such as solid heteropolyacids,^[17] proton conductivity can also be expected. The protons could come from hydrolysis of the water molecules attached to the lithium ions or from ionization of the oxothioanion; proton conduction would then proceed through proton exchange between water molecules, facilitated by the intricate hydrogen-bond network. Therefore, we have recorded complex impedance diagrams as a function of temperature, from -20°C to 50°C . Figure 7 shows a typical impedance plot. All diagrams

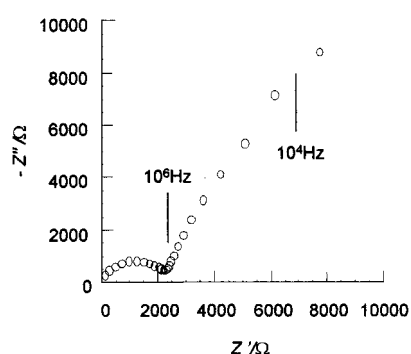


Figure 7. Typical impedance plot obtained at 20°C for an $\text{Li}_3\text{HMo}_8\text{W}\cdot 18\text{H}_2\text{O}$ pellet.

display an arc at high frequency associated with the bulk resistance, while the inclined spike at low frequency is ascribed to the relaxation phenomena at grain boundaries and blocking electrodes. The room temperature conductivity is equal to $2.2 \times 10^{-5} \text{ S cm}^{-1}$, a value slightly smaller than those observed for the best crystalline protonic^[17] or lithium conductors, such as solids with the NASICON structure, lithium rare earth titanium perovskites, or Li_3N phases, for which the conductivity at room temperature can reach $10^{-3} \text{ S cm}^{-1}$.^[18] The plot of $\log(\sigma)$ versus $1000/T$ (Figure 8) is linear only in the range -20°C to 20°C . In this temperature

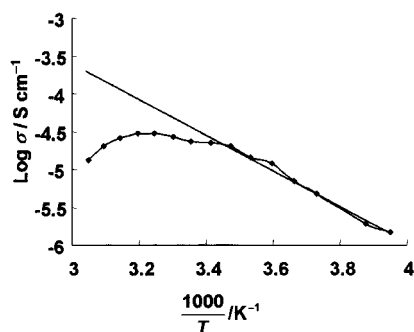


Figure 8. Arrhenius plot of the ionic conductivity between -20°C and 50°C with the calculated fit to the equation $\sigma = \sigma_0 \exp(-E_a/kT)$ only between -20°C and 20°C .

range, the fit of the conductivity to the equation $\sigma = \sigma_0 \exp(-E_a/kT)$ gives an activation energy E_a of 0.47 eV . At higher temperatures, the dehydration process shown by the thermogravimetric analysis explains the nonlinear behavior. The conductivity measurements on a single crystal (Table 3) show that there is not any privileged conduction path, as would be expected if the lithium ions were the main charge carriers. Furthermore, the values of the conductivity measured on a single crystal at room temperature are smaller by

Table 3. Comparison of the conductivities at 20°C and activation energies measured on a pressed pellet and a single crystal of $\text{Li}_3\text{HMo}_8\text{W}\cdot 18\text{H}_2\text{O}$.

	E_a [eV]	σ [S cm^{-1}]
pressed pellet	0.47	2.2×10^{-5}
single crystal		
large dimension	0.62	3.8×10^{-7}
medium dimension	0.61	1.8×10^{-7}
small dimension	0.72	3.8×10^{-7}

two orders of magnitude than those measured on a pressed powder sample; this suggests that the conduction mechanism in the powder involves an additional proton diffusion at the surface of grains. This hypothesis is also supported by the three-dimensional structure of $\text{Li}_3\text{HMo}_8\text{W}$; the neutron diffraction experiment has shown that the lithium ions were localized at room temperature, while the network of water molecules was highly disordered, thus facilitating proton diffusion. Ionic conductivity measurements correlated to weight changes will soon be performed under a controlled hygrometry atmosphere to clarify the conduction mechanism.

Conclusion

We have shown in this work that it was possible to synthesize in good yield, at room temperature, the new oxothiomolybdate anion $[\text{Mo}_8\text{S}_8\text{O}_8(\text{OH})_8\{\text{HWO}_5(\text{H}_2\text{O})\}]^{3-}$. This study opens the way to a new family of mixed $\text{Mo}^{\text{V}}/\text{W}^{\text{VI}}$ polyoxothioanions by varying the stoichiometry $[\text{Mo}_2\text{S}_2\text{O}_2]^{2-}/[\text{WO}_4]^{2-}$ and the pH of the medium. The lithium salt $\text{Li}_3[\text{Mo}_8\text{S}_8\text{O}_8(\text{OH})_8\{\text{HWO}_5(\text{H}_2\text{O})\}] \cdot 18\text{H}_2\text{O}$ is a pillared solid with partially filled lithium columns and a network of hydrogen-bonded water molecules conferring ionic conduction properties to the material. Preliminary studies have demonstrated that the neutral oxothiooctanuclear ring $\{\text{Mo}_8\text{S}_8\text{O}_8(\text{OH})_8\}$ can encapsulate various anionic templates such as $[\text{HMoO}_5(\text{H}_2\text{O})]^{3-}$, $[\text{H}_2\text{MoO}_5(\text{H}_2\text{O})]^{2-}$, and $[\text{C}_2\text{O}_4]^{2-}$, leading to the oxothio compounds Li_3HMo_9 , $\text{Li}_2\text{H}_2\text{Mo}_9$, and $\text{Li}_2\text{Mo}_8\text{ox}$. In the case of Mo_9 , the synthetic procedure gives control, through the pH of the solution, of the number of protons on the molecular ring and, hence, the number of counteranions in the structure. All these compounds exhibit the same remarkable three-dimensional structure, with occupancy factors for the lithium atoms in the lithium columns and the number of protons on the central template depending on the nature of the template and the charge of the anion. A complete study of the crystallographic structures as well as the

ionic conductivity properties of the whole family, including also the sodium, potassium, and rubidium salts, is under way and will be reported soon.

Experimental Section

Synthesis of $K_3[Mo_8S_8O_8(OH)_8(HWO_5(H_2O))] \cdot 18H_2O$ ($K_3HMo_8W \cdot 18H_2O$): As the $[Mo_2S_2O_2(OH)_4(H_2O)]^{2-}$ dithioanion was air-sensitive, the synthesis had to be carried out under a constant flow of N_2 gas. $Na_2WO_4 \cdot 2H_2O$ (0.18 g, 0.54 mmol) was dissolved in an aqueous solution of KOH (1M, 15 mL). The solution was degassed for 10 min and $\{K_{0.4}(NMe_4)_{0.1}I_{0.5}[Mo_2S_2O_2(OH)_2] \cdot 6.3H_2O\}_n$ [4, 5] (1.07 g, 2.0/n mmol) was added. The solution was stirred vigorously until the yellow precursor dissolved to give a dark red solution of $[Mo_2S_2O_2(OH)_4(H_2O)]^{2-}$. The pH was adjusted to 4.5 by dropwise addition of a solution of HCl (4M). The precipitation of the potassium salt was achieved by cooling the solution in an ice bath. The orange solid (0.92 g, 97.9%, based on Mo) was collected by filtration, washed with EtOH and dried with Et_2O . IR (KBr pellets): $\tilde{\nu} = 1060$ (w), 946 (s), 801 (w), 657 (s), 623 (m), 503 (s), 416 (w), 339 cm^{-1} (m); elemental analysis calcd (%) for $H_{47}K_3Mo_8O_{40}S_8W$: K 5.83, Mo 38.15, S 12.72, W 9.14; found: K 6.23, Mo 38.00, S 13.29, W 8.78.

Synthesis of $Li_3[Mo_8S_8O_8(OH)_8(HWO_5(H_2O))] \cdot 18H_2O$ ($Li_3HMo_8W \cdot 18H_2O$): K_3HMo_8W (0.5 g, 0.25 mmol) was dissolved in hot water (50 °C, 80 mL). After addition of LiCl (2 g, 47 mmol), the solution was allowed to stand at room temperature for crystallization. Orange crystals of $Li_3HMo_8W \cdot 18H_2O$ (0.45 g, 92.2% based on Mo), suitable for X-ray diffraction studies, were collected after several days. IR (KBr pellets): $\tilde{\nu} = 1063$ (w), 942 (s), 799 (w), 638 (s), 602 (m), 502 (s), 418 (w), 336 cm^{-1} (m); elemental analysis calcd (%) for $H_{47}Li_3Mo_8O_{40}S_8W$: Li 1.09, Mo 40.06, S 13.36, W 9.59; found: Li 1.01, Mo 39.75, S 12.75, W 9.29. A single crystal suitable for neutron diffraction was synthesized in similar conditions starting from more dilute solutions.

X-ray crystallography: Intensity data collection was carried out with a Siemens SMART three-circle diffractometer equipped with a CCD detector with MoK_{α} monochromatized radiation ($\lambda = 0.71073$ Å). The absorption correction was based on multiple and symmetry-equivalent reflections in the data set by using the SADABS program^[19] based on the method of Blessing.^[20] The structure was solved by direct methods and refined by full-matrix least-squares by using the SHELX-TL package.^[21] Crystallographic data are given in Table 4. Selected bond lengths are listed in Table 1.

Table 4. X-ray crystallographic and neutron diffraction data for $Li_3HMo_8W \cdot 18H_2O$.

	X-ray	Neutron
formula	$H_{47}Li_3Mo_8O_{40}S_8W$	
M_r [g]	1916.05	
crystal system	monoclinic	
space group	$C2/m$	
Z	2	
T [K]	296	
λ [Å]	0.71073	1.5365(2)
a [Å]	20.6576(9)	20.6754(9)
b [Å]	11.1379(5)	11.1509(5)
c [Å]	14.5642(7)	14.5769(7)
β [°]	133.891(1)	133.865(2)
V [Å ³]	2414.9(2)	2423.0(2)
ρ_{calcd} [g cm ⁻³]	2.635	2.614
μ [mm ⁻¹]	4.819	0.238
reflections collected	8451	2190
unique reflections (R_{int})	3250 (0.0361)	1685 (0.0241)
refined parameters	170	293
$R(F_o)^{[a]}$	0.0371	0.0635
$R_w(F_o^2)^{[b]}$	0.0918	0.1515

[a] $R1 = \sum |F_o| - |F_c| / \sum |F_c|$. [b] $wR2 = [\sum w(F_o^2 - F_c^2)^2 / \sum w(F_o^2)^2]^{1/2}$ with $1/w = \sigma^2 F_o^2 + aP^2 + bP$ and $P = F_o^2 + 2F_c^2/3$; $a = 0.049$, $b = 8.634$ for the X-ray refinement; $a = 0.075$, $b = 39.090$ for the neutron refinement.

Neutron diffraction experiment: A platelike orange-red single crystal of $Li_3HMo_8W \cdot 18H_2O$ of dimensions $1.5 \times 1.5 \times 0.8$ mm, volume 1.79 mm³, was glued to a 1 mm vanadium pin with Kwikfill and mounted on a Displex cryorefrigerator^[22] on the thermal-beam instrument D19 at Institut Laue–Langevin (ILL) equipped with a $4^\circ \times 64^\circ$ position-sensitive detector.^[23] The sample had a small satellite crystal with volume about 10% of the main crystal. The wavelength was 1.5365(2) Å from a Ge(115) monochromator in the reflection mode. The unique reflections to a 2θ value of 114° were measured at room temperature in equatorial geometry with ω scans, typically with 6 s per step. Reflections away from the equatorial plane were also included in the final data set (ILL programs Hklgen and Mad); Bragg intensities were integrated in three dimensions by using the ILL program Retreat.^[24] The space group $C2/m$ was confirmed. Three standard reflections were monitored on average every 12 hours and showed no significant variation, after rescaling the whole data set to constant time because of a deteriorating beam monitor. The unit cell dimensions were calculated from 1072 strong reflections (ILL program Rafd19). The intensities were corrected for attenuation by the cylindrical heat shields and by the crystal itself with the program D19abs, based on the ILL version of the CCSL system.^[25] The low values of the SHELX residuals $R(int)$ (0.024) and $R(sigma)$ (0.031) suggest that the data are well integrated in spite of the small parasitic crystal and the scaling to constant time. Occupation factors of the disordered oxygen and hydrogen atoms have been refined and subsequently fixed; disordered atoms were refined isotropically, all other atoms being refined anisotropically.

Further details on the crystal structure investigation may be obtained from the Fachinformationszentrum Karlsruhe, D-76344 Eggenstein-Leopoldshafen, Germany (fax: (+49) 7247-808-666; e-mail: crysdata@fiz-karlsruhe.de), on quoting the depository number CSD-412010 for the X-ray structure and CSD-412011 for the neutron structure.

Thermal analysis: TGA measurements were performed on powdered samples on a TA-Instrument 2050 thermo-analyser in air over the temperature range 25 to 250 °C (heating rate 5 °C min⁻¹). X-ray powder diffraction data were collected in air on a Siemens D5000 diffractometer (CoK_{α} radiation).

Lithium ion conductivity measurements: Two-probe impedance measurements were carried out by using an HP4192A impedancemeter between 10 and 10⁷ Hz. Impedance data were collected in the temperature range –20 to 50 °C, over cooling and heating cycles. Samples for electrical measurements were prepared as 13 mm diameter pellets of approximately 0.8 mm thickness ($\rho = 1.88$ g cm⁻³). The single crystal used for the conductivity measurements was a parallelepiped of approximate dimensions $1.5 \times 1.0 \times 0.5$ mm. Copper electrodes were applied by using Ag conducting paint. The bulk resistances were taken as the lowest point of the low frequency semicircle.

- [1] M. T. Pope, *Heteropoly and Isopoly Oxometalates*, Springer, Berlin, New York, 1983.
- [2] A. Dolbecq, D. Eisner, E. Cadot, F. Sécheresse, *Inorg. Chem.* **1999**, 38, 4217.
- [3] A. Müller, F. Peters, M. T. Pope, D. Gatteschi, *Chem. Rev.* **1998**, 98, 240.
- [4] E. Cadot, B. Salignac, J. Marrot, A. Dolbecq, F. Sécheresse, *Chem. Commun.* **2000**, 261.
- [5] E. Cadot, B. Salignac, S. Halut, F. Sécheresse, *Angew. Chem.* **1998**, 110, 631; *Angew. Chem. Int. Ed.* **1998**, 37, 612.
- [6] a) A. Dolbecq, B. Salignac, E. Cadot, F. Sécheresse, *Bull. Pol. Acad. Sci.* **1998**, 46, 237; b) B. Salignac, S. Riedel, A. Dolbecq, F. Sécheresse, E. Cadot, *J. Am. Chem. Soc.* **2000**, 122, 10381.
- [7] a) E. Cadot, A. Dolbecq, B. Salignac, F. Sécheresse, *Chem. Eur. J.* **1999**, 5, 2396; b) E. Cadot, B. Salignac, T. Loiseau, A. Dolbecq, F. Sécheresse, *Chem. Eur. J.* **1999**, 5, 3390.
- [8] F. Sécheresse, E. Cadot, A. Dolbecq, *J. Solid State Chem.* **2000**, 152, 78.
- [9] E. Cadot, A. Dolbecq, B. Salignac, F. Sécheresse *J. Phys. Chem. Solids* **2001**, 62, 1533.
- [10] A. Dolbecq, E. Cadot, F. Sécheresse, *Chem. Commun.* **1998**, 2293.
- [11] a) A. G. Orpen, L. Brammer, F. H. Allen, O. Kennard, D. G. Watson, R. Taylor, *J. Chem. Soc. Dalton Trans.* **1989**, S1; b) F. Corazza, C. Floriani, A. Chiesi-Villa, C. Guastini, *J. Chem. Soc. Chem. Commun.* **1990**, 640.

- [12] M. T. Pope, M. G. M. Varga, Jr., *J. Chem. Soc. Chem. Commun.* **1966**, 653.
- [13] a) M. G. Walawalkar, R. Murugavel, A. Voigt, H. W. Roesky, H.-G. Schmidt, *J. Am. Chem. Soc.* **1997**, *119*, 4656; b) G. Müller, G.-M. Maier, M. Lutz, *Inorg. Chim. Acta* **1994**, *218*, 121; c) L. R. Falvello, J. Forniés, E. Lalinde, A. Martín, T. Moreno, J. Sacristán, *Chem. Commun.* **1998**, 141.
- [14] J. P. Declercq, J. Feneau-Dupont, J. Ladriere, *Polyhedron* **1993**, *12*, 1031.
- [15] N. N. Greenwood, A. Earnshaw, *Chemistry of the Elements*, Pergamon, New-York (USA), **1984**.
- [16] G. A. Jeffrey, W. Saenger, *Hydrogen Bonding in Biological Structures*, Springer, Berlin (Germany), **1991**.
- [17] a) E. A. Ukshe, L. S. Leonova, A. I. Korosteleva, *Solid State Ionics* **1989**, *36*, 219; b) Q. Wu, G. Meng, *Solid State Ionics* **2000**, *136–137*, 273.
- [18] A. D. Robertson, A. R. West, A. G. Ritchie, *Solid State Ionics* **1997**, *104*, 1.
- [19] G. M. Sheldrick, SADABS, Program for Scaling and Correction of Area Detector Data, University of Göttingen, Göttingen (Germany), **1997**.
- [20] R. Blessing, R. *Acta Crystallogr. Sect. A* **1995**, *51*, 33.
- [21] a) G. M. Sheldrick, *Acta Crystallogr. Sect. A* **1990**, *46*, 467; b) G. M. Sheldrick, SHELX-TL version 5.03, Software Package for the Crystal Structure Determination, Siemens Analytical X-ray Instrument Division, Madison, WI (USA), **1994**.
- [22] J. Archer, M. S. Lehmann, *J. Appl. Crystallogr.* **1986**, *19*, 456.
- [23] M. Thomas, R. F. D. Stansfield, M. Berneron, A. Filhol, A., G. Greenwood, G., J. Jacobe, D. Feltin, S. A. Mason in *Position-Sensitive Detection of Thermal Neutrons* (Eds.: P. Convert, J. B. Forsyth), Academic Press, London, **1983**, p. 344.
- [24] C. Wilkinson, H. W. Khamis, R. F. D. Stansfield, G. J. McIntyre, *J. Appl. Crystallogr.* **1988**, *21*, 471.
- [25] J. C. Matthewman, P. Thompson, P. J. Brown, *J. Appl. Crystallogr.* **1982**, *15*, 167.

Received: August 1, 2001 [F3462]